The liquid–vapour interface of chain molecules investigated using a density functional approach

2004 J. Phys.: Condens. Matter 16 8861

(http://iopscience.iop.org/0953-8984/16/49/005)

INSTITUTE OF PHYSICS PUBLISHING JOURNAL OF PHYSICS: CONDENSED MATTER

J. Phys.: Condens. Matter **16** (2004) 8861–8873 PII: S0953-8984(04)84797-0

The liquid–vapour interface of chain molecules investigated using a density functional approach

P Bryk, K Bucior, S Sokołowski and G Żukociński

Department for the Modelling of Physico-Chemical Processes, Maria Curie-Skłodowska University, 20-031 Lublin, Poland

Received 10 August 2004, in final form 26 October 2004
Published 26 November 2004
Online at stacks.iop.org/JPhysCM/16/8861
doi:10.1088/0953-8984/16/49/005

Abstract

A microscopic density functional theory is used to investigate the liquid–vapour interface of fluids composed of short linear chains. We analyse the structure of the interface and evaluate the dependence of the surface tension and of the interfacial width on the temperature. The difference in chain length leads to differences in the thermodynamic properties of the fluids. The liquid-phase parts of the interfacial profiles of shorter chains exhibit oscillations at low temperatures. These oscillations vanish for longer chains. The surface tension and the interfacial width at a given temperature are found to increase with the chain length. Both the surface tension and the interfacial width scale as power laws upon approaching the critical point with critical exponents characteristic of mean-field-type theories and with prefactors depending on the chain length only.

1. Introduction

A detailed knowledge of physical and structural properties of molecular fluids is an essential prerequisite from the point of view of both theory and application. In particular, interfacial behaviour of complex fluids plays an important role in chemical engineering and the knowledge of surface tension is important for development and design of several processes of industrial importance. Of course, direct experiments [1–7] leading to the evaluation of the phase diagrams and the values of surface tension are always preferred over more or less approximate theoretical approaches. However, reliable measurements are not always readily available or feasible. In addition, some of the structural properties are very difficult to access experimentally. Several statistical mechanical methods, developed recently for complex fluids, have proved to be very successful in probing properties and investigating phenomena that are difficult or impossible to study by means of experiment.

Any strategy for developing a theory of molecular fluids begins from microscopic principles and then resolves the problem either by carrying out numerical simulations or

by introducing approximations that convey physical insight and reduce computational effort. Several equations of state developed for molecular liquids and their mixtures predict accurately thermodynamic properties and phase equilibria of bulk fluids; see e.g. [8–17]. An important contribution in this area has been the development of the so-called statistical associating fluid theory (SAFT) and its many extensions [18–21]. A good example of the versatility of the SAFT approach in describing the thermodynamic properties of bulk non-polar and polar fluids has been provided by Huang and Radosz [22, 23], who have extended the SAFT approach to many real, molecular and macromolecular fluids such as chain, aromatic, and chlorinated hydrocarbons, ethers, alkanols (aliphatic alcohols), carboxylic acids, esters, ketones, amines, and low-weight polymers. In the case of mixtures just one binary, temperature-independent parameter was sufficient to reproduce with a good accuracy experimental data that are difficult to predict from equations of state.

SAFT is based on the first-order perturbation theory of Wertheim [24]. It was originally developed for chains formed from Lennard-Jones fluids with the structure of the hard-sphere fluid as a reference [18–20]. Subsequently, several efforts have been undertaken to incorporate a more accurate description of the reference Lennard-Jones monomeric fluid, as well as to describe polar molecules and polymers [25–30]. The ideas of SAFT have also been incorporated into microscopic theories of *nonuniform* molecular fluids.

Density functional (DF) approaches are probably the most successful and widespread theories of nonuniform fluids. Their predictions are usually more accurate and require much less computational effort than other theories of nonuniform fluids [31, 32]. In DF methods the thermodynamic properties of the system are expressed as functionals of the spatially varying single-particle density [33]. Several density functional studies have been devoted to the description of nonuniform associating fluids [34–36] and, in particular, to investigation of the liquid–vapour interface of associating fluids [37–42].

Wertheim's ideas have also been employed to develop DF theories aiming at the description of nonuniform fluids composed of molecules that are built of spherical segments bonded permanently together via short-range, strong attractive associative forces. A special case is a fluid consisting of chain molecules. One of the first approaches towards description of such systems was proposed by Kierlik and Rosinberg [43]. An alternative density functional description of nonuniform chain fluids was developed by Yu and Wu [44, 45]. Müller *et al* [46–48] reported the results of Monte Carlo, density functional, and self-consistent field (SCF) theory investigations of surface and interfacial properties of a molecular fluid composed of short linear chains (built of ten segments). Their approach was based on a model according to which the molecules are treated as spherical sites connected by springs, and with site–site and site–surface interactions of a Lennard-Jones type. Theoretical results obtained by Müller *et al* [46–48] agreed well with computer simulations. However, they also required much computational effort. This is due to the fact that within the SCF approach the problem of many mutually interacting inhomogeneous chains is approximated by that of a single chain in a self-consistently determined field that mimics the effect of interactions with neighbouring molecules. This single-chain problem is solved using partial enumeration over a large number of chain conformations extracted from simulations [49]. The enumerations were performed in parallel on a CRAY T3E machine. Consequently, extensive studies of interfacial phenomena within the framework of SCF theory would be rather time-consuming.

In this work we apply the density functional theory of Yu and Wu [44, 45] to study the liquid–vapour interface for systems of molecules built of freely jointed tangential Lennard-Jones segments. Since the numerical implementation of the latter theory is less involved than that of Müller *et al* we are able to cover a wide range of the molecular parameters. The main purpose of the present work is to investigate the structure of an interface and the surface tension

of molecules built of up to 32 segments. A mean-field approximation is applied to calculate the contribution to the free energy functional arising form the attractive segment–segment interaction.

The calculation of liquid–vapour density profiles and surface tensions requires knowledge of the bulk phase diagrams for the fluids in question. Numerous calculations of the bulk thermodynamic properties for models similar to that applied here have been reported in the literature; see e.g. [48, 50, 51, 14, 15, 16]. However, despite the similarity of the approach, some details are different in our theory. Our surface calculations are preceded by calculations of the bulk phase equilibria. We must stress, however, that the goal of our calculations is not to obtain results that one could quantitatively compare with experimental data for particular fluids. Rather, we focus on the application of the theory without any adjustable parameters in order to extract the general features observed for that class of molecular fluids. An analogous theory can be used to describe adsorption of chain-like molecules on solid surfaces and to study phenomena such as wetting [52], layering, and capillary condensation. If our approach is able to describe the general trends observed for the liquid–vapour interface of short-chain fluids, then one could expect the theory to be at least qualitatively reliable in describing confined systems.

2. Theory

The theory outlined below describes thermodynamic and structural properties of an interface between the liquid and vapour phases of chain particles. The fluid molecules are built of M spherical segments, which are tangentially jointed by a bonding potential acting between the adjacent segments of the same chain. In principle, the theory can be written down for the general case of segments of different sizes and interactions. However, we assume here that all the segments can be modelled by hard spheres of identical diameter σ with additional short-ranged attractive interactions. Overlap between any two segments is excluded [44, 53].

The bonding potential, $V_b(\mathbf{R})$, is a sum of the potentials v_b between the adjacent segments:

$$V_b(\mathbf{R}) = \sum_{j=1}^{M-1} v_b(|\mathbf{r}_{j+1} - \mathbf{r}_j|). \tag{1}$$

In the above $\mathbf{R} \equiv (\mathbf{r}_1, \mathbf{r}_2, \ldots, \mathbf{r}_M)$ is the set of segment positions. The bonding potential satisfies the relation

$$\exp[-\beta V_b(\mathbf{R})] = \prod_{j=1}^{M-1} \delta(|\mathbf{r}_{j+1} - \mathbf{r}_j| - \sigma)/4\pi\sigma^2. \tag{2}$$

We also introduce an attractive interaction between the segments of the form

$$u(r) = \begin{cases} 0 & \text{for } r \leqslant \sigma \\ 4\varepsilon\left[(\sigma/r)^{12} - (\sigma/r)^6\right] & \text{for } \sigma < r \leqslant r_{\text{cut}} \\ 0 & \text{for } r > r_{\text{cut}}, \end{cases} \tag{3}$$

where r_{cut} is the cut-off distance. The energy parameter ε is independent of the interacting segment index. The form of the potential (3) excludes the interaction between the adjacent segments within the same chain. Therefore the attractive potential energy comes from the interactions between the two segments belonging to different chains as well as from the interactions between the two non-neighbouring segments within the same chain.

The above model differs from those described in [46–48, 51]. In our approach we assume that the bonding potential, v_b, is of infinitely short range, whereas Müller and co-workers used

the so-called finitely extensible nonlinear elastic potential, responsible for the connectivity between the adjacent segments.

Following Yu and Wu [44], an interface between the fluid and vapour phases is described by defining the grand potential of the system Ω as a functional of the local density of the fluid, $\rho(\mathbf{R})$,

$$\Omega[\rho(\mathbf{R})] = F_{\mathrm{id}}[\rho(\mathbf{R})] + F_{\mathrm{ex}}[\rho(\mathbf{R})] + F_{\mathrm{att}}[\rho(\mathbf{R})] + \int \mathrm{d}\mathbf{R}\, \rho(\mathbf{R})(V_{\mathrm{ext}} - \mu), \quad (4)$$

where μ is the chemical potential, F_{id} is the ideal part of the Helmholtz free energy,

$$\beta F_{\mathrm{id}}[\rho(\mathbf{R})] = \beta \int \mathrm{d}\mathbf{R}\, \rho(\mathbf{R}) V_{\mathrm{b}}(\mathbf{R}) + \int \mathrm{d}\mathbf{R}\, \rho(\mathbf{R})[\ln(\rho(\mathbf{R})) - 1], \quad (5)$$

F_{att} is the free energy due to attractive forces between the molecules, whereas the excess free energy of the hard-sphere chains, F_{ex}, is a sum of the contribution resulting from the hard-sphere repulsion between segments, F_{HS}, and the contribution due to the chain connectivity, F_{C}. We assume further that both F_{ex} and F_{att} are functionals of the average segment density only, defined as

$$\rho_{\mathrm{s}}(\mathbf{r}) = \sum_{j=1}^{M} \rho_{\mathrm{s},j}(\mathbf{r}) = \sum_{j=1}^{M} \int \mathrm{d}\mathbf{R}\, \delta(\mathbf{r} - \mathbf{r}_j)\rho(\mathbf{R}), \quad (6)$$

where $\rho_{\mathrm{s},j}(\mathbf{r})$ is the local density of segment j of the chain. Each of the components, F_α, $\alpha =$ HS or C, is expressed as a volume integral: $F_\alpha = \int \Phi_\alpha(\mathbf{r})\, \mathrm{d}\mathbf{r}$.

The hard-sphere contribution is evaluated from fundamental measure theory (FMT) [54–56]:

$$\Phi_{\mathrm{HS}} = -n_0 \ln(1 - n_3) + \frac{n_1 n_2 - \mathbf{n}_{V1} \cdot \mathbf{n}_{V2}}{1 - n_3} + n_2^3 (1 - \xi^2)^3 \frac{n_3 + (1 - n_3)^2 \ln(1 - n_3)}{36\pi n_3^2 (1 - n_3)^2}, \quad (7)$$

where $\xi(\mathbf{r}) = |\mathbf{n}_{V2}(\mathbf{r})|/n_2(\mathbf{r})$.

The contribution Φ_{C} results from Wertheim's first-order perturbation theory [24]:

$$\Phi_{\mathrm{C}} = \frac{1 - M}{M} n_0 \zeta \ln[y_{\mathrm{HS}}(\sigma)], \quad (8)$$

where $\zeta = 1 - \mathbf{n}_{V2} \cdot \mathbf{n}_{V2}/(n_2)^2$ and the contact value of the hard-sphere radial distribution function, y_{HS}, is obtained from the Carnahan–Starling equation of state:

$$y_{\mathrm{HS}}(\sigma) = \frac{1}{1 - n_3} + \frac{n_2 \sigma \zeta}{4(1 - n_3)^2} + \frac{(n_2 \sigma)^2 \zeta}{72(1 - n_3)^3}. \quad (9)$$

The definition of weighted densities, n_α, $\alpha = 0, 1, 2, 3, V1, V2$ is given in [54].

To complete the theory we write down the mean-field attractive potential contribution to the free energy:

$$F_{\mathrm{att}} = \tfrac{1}{2} \int \mathrm{d}\mathbf{r}\, \mathrm{d}\mathbf{r}'\, u(|\mathbf{r} - \mathbf{r}'|)\rho_{\mathrm{s}}(\mathbf{r})\rho_{\mathrm{s}}(\mathbf{r}'). \quad (10)$$

We stress that the last equation is valid under the condition that all the segments are identical. Since our approach uses FMT-style weighted densities, it clearly belongs to the non-local class of DF theories. Consequently short-ranged features of the density profiles such as the oscillations in the vicinity of the interface should be captured.

The density profile $\rho(\mathbf{R})$ between the liquid and vapour phases is determined by minimizing the grand potential, $\delta\Omega[\rho(\mathbf{R})]/\delta\rho(\mathbf{R}) = 0$. This condition leads to

$$\rho(\mathbf{R}) = \exp\left\{\beta\mu - \beta V_{\mathrm{b}}(\mathbf{R}) - \beta \sum_{j=1,M} \lambda_j(\mathbf{r}_j)\right\}, \quad (11)$$

where

$$\lambda_j(\mathbf{r}_j) = \frac{\delta\,[F_{\rm ex} + F_{\rm att}]}{\delta\rho_{\rm s}(\mathbf{r}_j)} + v_j(\mathbf{r}_j). \tag{12}$$

From equations (6) and (11) we obtain the equation for the average segment local density:

$$\rho_{\rm s}(\mathbf{r}) = \exp(\beta\mu) \int {\rm d}\mathbf{R} \sum_{j=1}^{M} \delta(\mathbf{r} - \mathbf{r}_j) \exp\left[-\beta \sum_{l=1}^{M} \lambda_l(\mathbf{r}_l)\right]. \tag{13}$$

In the planar geometry $\rho(\mathbf{r}) \equiv \rho(z)$, so equation (13) can be rewritten as

$$\rho_{\rm s}(z) = \exp(\beta\mu) \sum_{j=1}^{M} \exp[-\beta\lambda_j(z)] G_j(z) G_{M+1-j}(z), \tag{14}$$

where the functions $G_j(z)$ are calculated from the recurrence relation

$$G_j(z) = \begin{cases} 1 & \text{for } j = 1 \\ \displaystyle\int {\rm d}z'\, \exp[-\beta\lambda_j(z')] \frac{\theta(\sigma - |z - z'|)}{2\sigma} G_{j-1}(z') & \text{for } 1 < j < M \end{cases} \tag{15}$$

with θ being the step function. Equations (14) and (15) were solved using the standard Picard iterative method.

3. Results and discussion

Before considering the liquid–vapour interface we have evaluated the bulk phase diagrams. If the local density is constant, the grand potential of the system can be calculated analytically. The bulk phase equilibria (the binodals) were evaluated by imposing equality of the chemical potentials and the pressure p in the coexisting phases. The spinodal lines delimiting the regions that are stable against fluctuations were evaluated by solving the equation $\partial p/\partial\rho = 0$ [57].

Unless stated otherwise, we use standard definitions of the reduced quantities, i.e. $T^* = k_{\rm B}T/\varepsilon$, $\rho^*_\alpha = \rho_\alpha\sigma^3$ (where α stands for any index), $z^* = z/\sigma$, etc. All the calculations were carried out setting the cut-off distance (see equation (3)) to $r_{\rm cut} = 3\sigma$.

We begin with the presentation of the bulk phase diagrams. Figure 1 shows examples of the liquid–vapour coexistence envelopes (solid curves) in the reduced bulk segment density $\rho^*_{\rm b} = \rho_{\rm s,b}\sigma^3$–reduced temperature plane for chains of different lengths (shown in the figure). For some selected chain lengths we have also included the spinodal lines (dotted curves). The locations of the critical points are marked by diamonds. As the chain length increases the critical temperature increases whereas the critical density decreases.

Although a direct comparison against existing experimental results is beyond the scope of the present work, it is instructive to compare general trends stemming from our theory with other approaches available in the literature. In figure 2(a) we show a comparison of the critical temperatures resulting from the present approach (open circles) with the data reported in [15, 32, 58]. To make such comparison possible, we have divided the temperatures by the critical temperature of the monomer fluid, $T_{\rm c}(M = 1)$. The critical temperatures evaluated in the above-cited works were obtained from different approaches. In particular, Pamies and Vega [15] used SAFT theory (open squares), Miqueu *et al* [32] used a volume-corrected Peng–Robinson equation of state (black dots), whereas the approach of Penfold *et al* [58] was based on the application of effective spherically symmetric interparticle potentials (asterisks). The aim of all these studies was to fit the experimental [59–61] or simulation [62, 63] data and thus they introduced some adjustable parameters. The theory used in the present work, however,

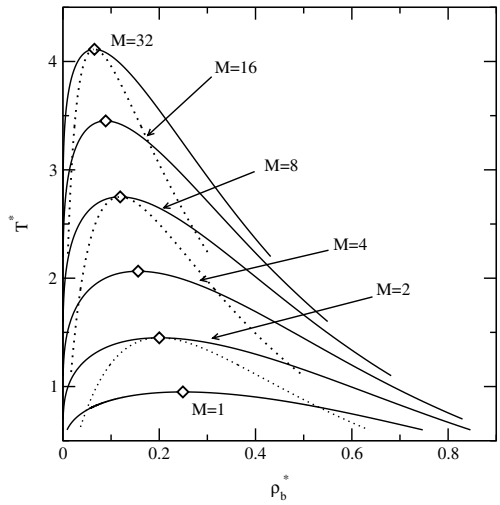

Figure 1. Examples of liquid–vapour phase diagrams of M-mers in the segment density–temperature plane. Critical points are marked by diamonds. Solid curves denote binodals whereas dotted curves denote spinodals. The values of M are given in the figure.

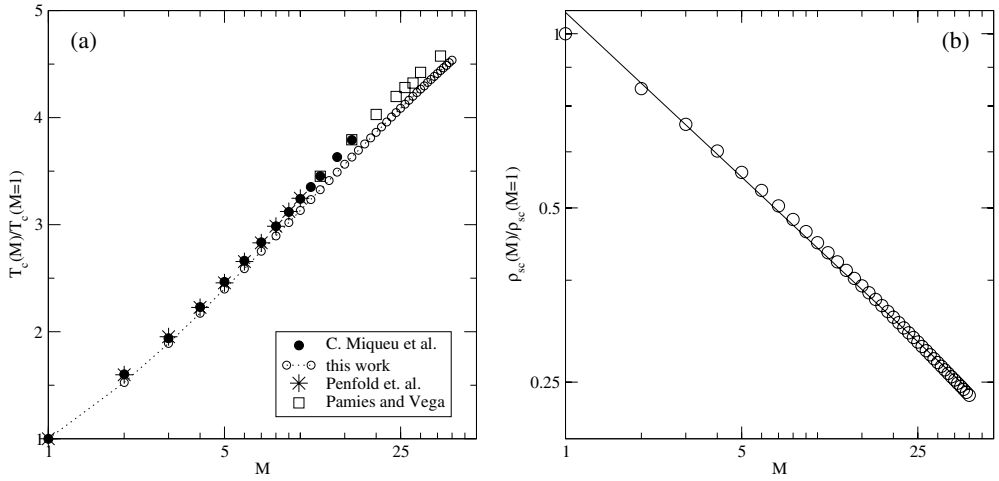

Figure 2. (a) A comparison of the literature data of Pamies and Vega [15], Miqueu *et al* [32], Penfold *et al* [58], and the results of the present approach (circles and dotted curve) for the dependence of the critical temperatures $T_c(M)/T_c(M = 1)$ on M. (b) The dependence of the critical segment density on M. Points denote theoretical results, the line the approximation with the power law (see the text).

does not involve such parameters. Therefore, we can conclude that the agreement observed in figure 2(a) is quite satisfactory.

Several formulae have been proposed in the literature for scaling the critical properties of alkanes with the number of carbon atoms in the molecule (i.e. with the number of segments in the present approach). For example, Wilding *et al* [64] proposed a general expression $\theta_c = 1/(c_1 + c_2 M^x)$, where θ_c represents any of the critical properties. However, analysing the data from figure 2(a) we have found that the critical temperature for the fluid of

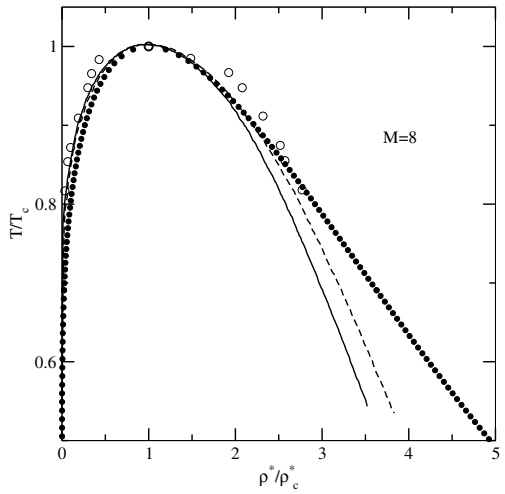

Figure 3. The liquid–vapour coexistence curve of octamers in the reduced temperature T/T_c–reduced density, ρ/ρ_c plane (T_c and ρ_c denote the critical temperature and density, respectively). Black circles result from the present approach, open circles are the results of computer simulations [65], and solid and dashed curves are the results of SAFT calculations [15].

molecules of M segments, $T_c(M)$, scales well with $T_c(M)/T_c(1) \propto \ln(M)$ ($T_c(M)/T_c(1) = 0.7586 + 1.031\ln(M)$). For $2 \leqslant M \leqslant 40$ the correlation coefficient is as high as $R^2 = 0.9996$. Performing similar comparisons for the critical densities is difficult, because the calculation of the reduced densities from the experimental data requires additional assumptions about the molecular size parameter. We only note that the critical segment density, $\rho_{sc}(M)$, can be quite well approximated by the power law $\rho_{sc}(M)/\rho_{sc}(M=1) = AM^B$ with the exponent $B = -0.4071$ and the prefactor A very close to unity ($A = 1.088$); see figure 2(b). The correlation coefficient for this relation is also very high, $R^2 = 0.998$.

Figure 3 compares the liquid–vapour envelope for octamers (n-octane). Black circles denote the results of the present theory, open circles the results of simulations [65], and solid and dashed curves the SAFT theory results of Pamies and Vega [15], obtained by using the Johnson *et al* [66] and Kolafa and Nezbeda [67] equation of state for the reference fluid (for the details see [15]). Following previous works (see figure 4 in [58]) we have used the temperature–density representation reducing each variable by its critical value. At higher temperatures ($T/T_c > 0.8$) the agreement of the present theory with computer simulations is not worse than the agreement of the SAFT results. At lower temperatures, however, the predictions of our approach are less satisfactory.

Summarizing the results obtained for the bulk systems, the model applied in the present paper gives reasonable phase diagrams and critical properties of short-chain fluids. It agrees qualitatively with semi-empirical approaches that involve adjustable parameters.

Let us discuss now the structure of the liquid–vapour interface. In figure 4 we show examples of the average segment density profiles (see equation (14)) evaluated across the liquid–vapour interface. In each part of this figure the highest temperature is very close to the critical temperature. The profiles evaluated at these temperatures are very diffuse and the interfacial regions extend over many segment diameters. At low temperatures, however, the interface is narrow. We return to the problem of the interfacial width below.

At the lowest temperatures investigated the liquid parts of the profiles exhibit oscillatory behaviour close to the interface. It is interesting that the oscillations are larger for dimers

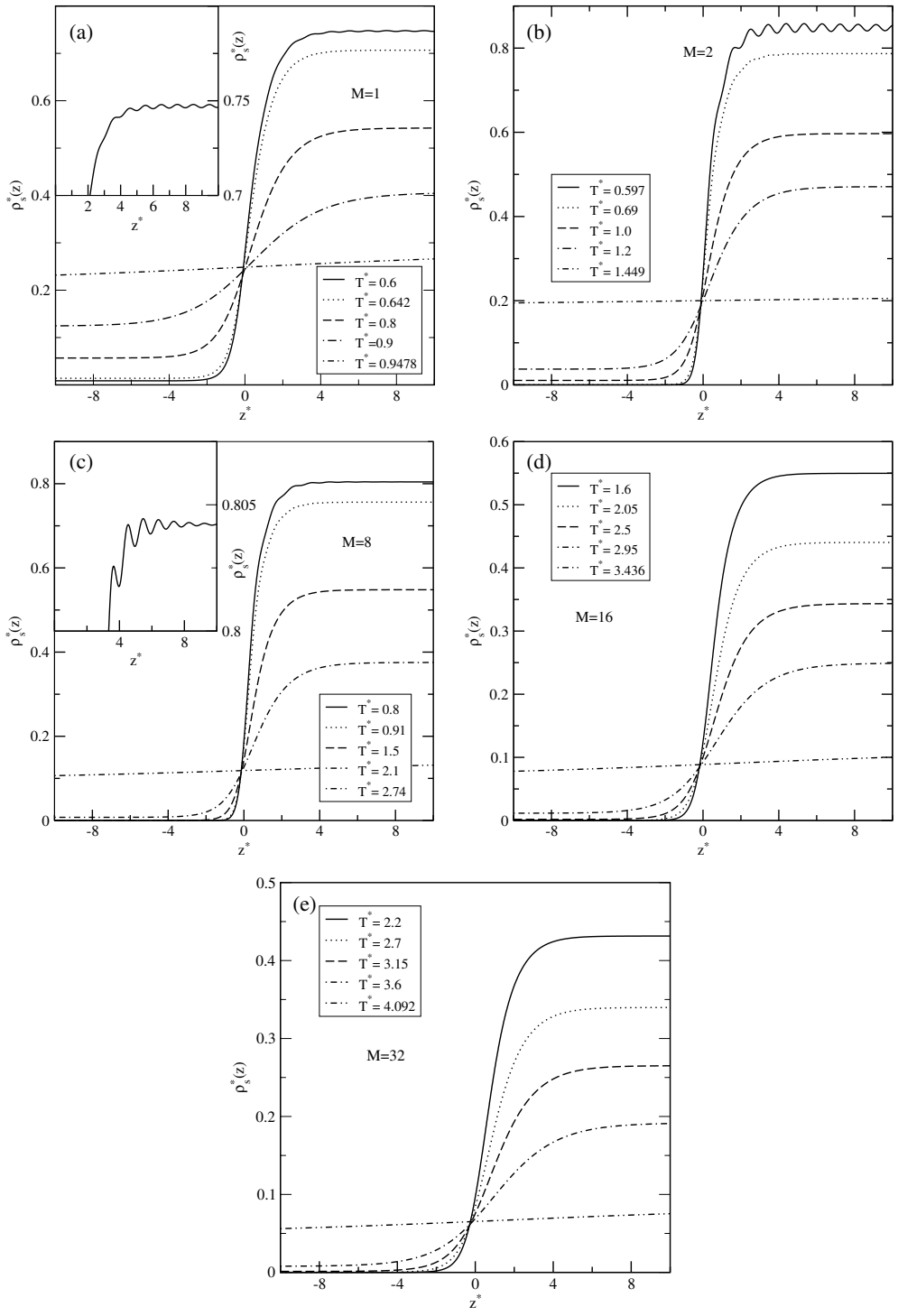

Figure 4. Liquid–vapour density profiles at different reduced temperatures, $T^* = kT/\varepsilon$. Consecutive parts are for $M = 1$, 2, 8, 16 and 32, respectively. Insets to figures (a) and (c) show the liquid profiles close to the interface at the lowest temperature. The distance is measured in segment diameters, $z^* = z/\sigma$.

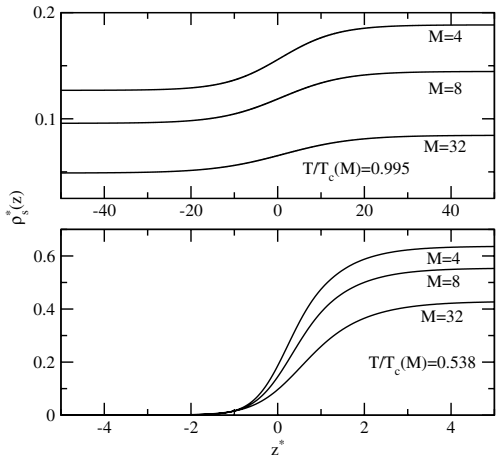

Figure 5. Average segment density profiles for $M = 4$, 8, and 32 at identical reduced temperatures $T/T_c(M)$. The upper panel shows profiles of systems that are very close to the bulk critical temperature, the lower panel ones at relatively low temperature.

(figure 4(b)) than for monomers (figure 4(a)). However, a further increase in the number of segments diminishes the oscillations and for $M = 8$ their magnitude is small (see figure 4(c)). For $M \geqslant 16$ the oscillations vanish, even at quite low temperatures $T/T_c(M)$ (see figures 4(d) and (e)). Also, for any M no oscillations in the gas-phase part of the profiles are observed. To get a deeper insight into the crossover of the density profile decay from smooth (exponential) to oscillatory it would be useful to evaluate the Fisher–Widom line [68]. However, for the theory in question this is not a simple task and we postpone the solution of this problem to future work.

Figure 5 compares the profiles for $M = 4$, 8, and 32 at identical reduced temperatures, $T/T_c(M)$. The lower panel shows the profiles at a low reduced temperature, $T/T_c(M) = 0.538$. Instantaneously, this temperature is high enough to prevent the occurrence of oscillations on the liquid part of the profile. One observes that the interfacial width increases with increase of M.

The theory allows us to evaluate the density distribution of particular segments within the molecule. Obviously, because of the molecular symmetry, the profiles of segments i and $M-i+1$ are identical. In figure 6 we show examples of the middle-segment (solid curves) and end-segment (dashed curves) profiles for $M = 8$ (upper panel) and for $M = 32$ (lower panel). The calculations have been carried out at the lowest temperatures from figure 4. For $M = 8$ the liquid parts of the profiles exhibit oscillatory behaviour, similarly to the averaged profiles from figure 4. There is a shift in both profiles and the oscillations are more pronounced in the middle-segment density profiles. The width of the interfacial region is larger for the end than for the middle segments. Similar structure of the interface was observed in binary polymer melts [53]. However, within our approach it is not possible to draw any conclusion concerning the orientational ordering of the molecules at the interfaces. Note that no such ordering was found in simulations of short chains at the liquid–vapour interface [69].

Quantitatively the width of the interfacial zone can been characterized by the parameter W, defined as [70]

$$W = -[\rho_s(z = Z) - \rho_s(z = -Z)] \left[\frac{\mathrm{d}\rho_s(z)}{\mathrm{d}z} \right]^{-1}_{z=z_0}, \tag{16}$$

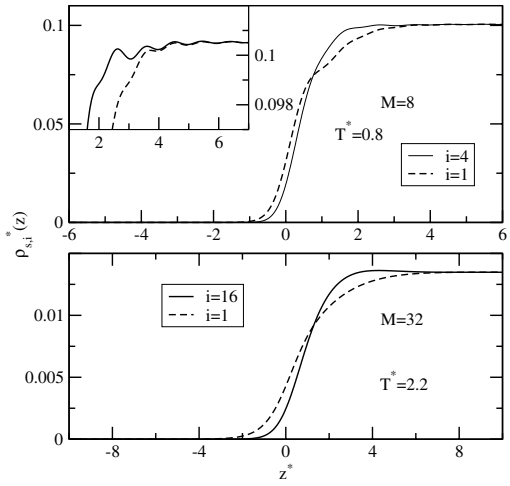

Figure 6. Middle-segment and end-segment density profiles for $M = 8$ (upper panel) and $M = 32$ (lower panel). All the parameters are given in the figure. The inset to the upper panel magnifies the liquid-phase part of the profiles.

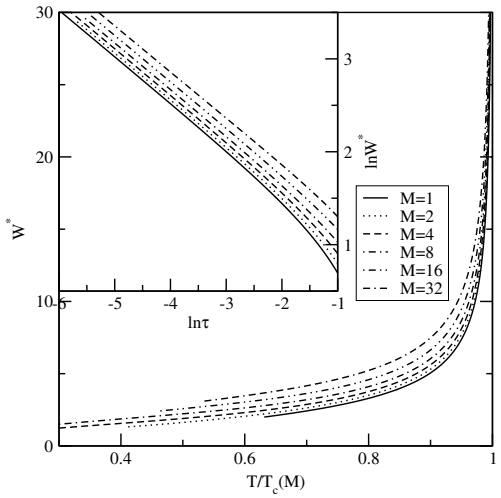

Figure 7. The dependence of the interfacial width on the temperature, reduced by the critical temperature, $T/T_c(M)$. The inset illustrates the divergence of the interfacial width. The slope of the linear parts of the log–log plots is -0.5.

where z_0 is given by $\rho_s(z_0) = (1/2)[\rho_s(z = Z) + \rho_s(z = -Z)]$ and $\rho_s(z = Z)$ and $\rho_s(z = -Z)$ are the segment densities of the coexisting liquid and vapour phases. In figure 7 we show the dependence of $W^* = W/\sigma$ upon the temperature. We see that at a fixed value of T/T_c the interface becomes wider as M increases. As the temperature approaches the critical temperature, the interfacial width diverges (in the same manner as the correlation length). To investigate the character of this divergence, we have plotted the values of $\ln W^*$ versus $\ln \tau = \ln(1 - T/T_c(M))$; see the inset to figure 7. For T approaching the critical temperature the dependence of $\ln W^*$ on $\ln \tau$ is linear. The straight lines obtained for different values of M run parallel. We have found the following scaling: $W^* \sim \tau^{-\nu}$ with $\nu = 0.5$. This

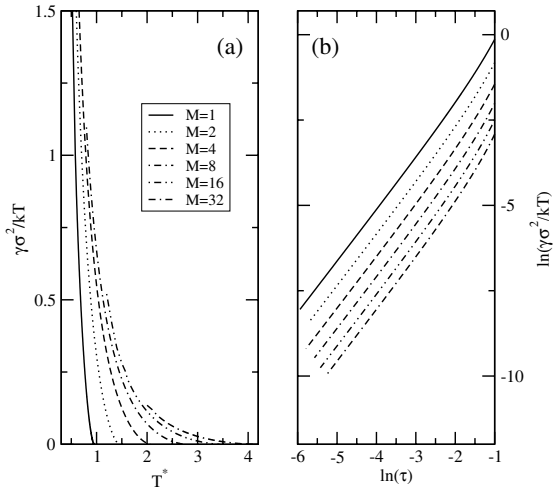

Figure 8. The dependence of the surface tension on temperature, $T^* = kT/\varepsilon$ (a), and the corresponding log–log plots (b). The slope of the linear parts of the curves in (b) is 1.5.

value of the exponent is characteristic of a mean-field-type theory [71]. This finding is not surprising because both the free energy contribution arising from chain interconnectivity and the free energy contribution due to attractive segment–segment interactions are of the mean-field type [53]. Therefore one can write $W^* = f_1(M)\tau^{-\nu}$ with $f_1(M)$ being a function of the chain length only.

Finally, figure 8 shows the results of surface tension calculations. The values of the surface tension are directly obtained from the present theory as the difference between the grand potentials per unit area of the interfacial system and the bulk, $\gamma = \Omega - \Omega_b$. The calculations were carried out for different values of M. Figure 8(a) shows the scaling of the surface tension with the temperature whereas figure 8(b) shows the scaling in the critical region using appropriate scaling variables. We find that at a given temperature the surface tension increases with the chain length. However, when the surface tensions for fluids with different chain lengths are measured at the same rescaled temperature, i.e. at the same 'distance' from the critical point (see figure 8(b)), the trend is reversed, i.e. the surface tension decreases with increase of the chain length. It is well known that the surface tension vanishes as $\gamma^* \sim \tau^{(d-1)\nu}$ upon approaching the critical point [71]. Within a mean-field type of theory one has $d = 4$ and $\nu = \frac{1}{2}$, so the surface tension should vanish with an exponent $\frac{3}{2}$ and this is confirmed by our numerical calculations (see figure 8(b)). Similarly to the case for the interfacial width, one can write $\gamma^* = f_2(M)\tau^{(d-1)\nu}$ with $f_2(M)$ being a function of the chain length only.

4. Summary

We have carried out studies of bulk and interfacial properties of fluids composed of different numbers of tangentially jointed spherical segments. The difference in chain length leads to differences in the thermodynamic properties of the fluids. The liquid-phase parts of the interfacial profiles of shorter chains exhibit oscillations at low temperatures. These oscillations vanish for longer chains. The interfacial width is found to increase with the chain length. Likewise, we find that at a given temperature the surface tension increases with M. Both the surface tension and the interfacial width scale as power laws upon approaching the critical

point with critical exponents characteristic of theories of a mean-field type with prefactors depending on the chain length only.

There are several factors influencing the accuracy of the theory. For example, the associative free energy is evaluated assuming that the radial distribution function is that of a hard-sphere reference fluid. It has been demonstrated [72] that in the case of a dimerizing fluid the replacement of the hard-sphere radial distribution function by a more sophisticated approximation improves the agreement with simulation data. In principle, it should also be possible to implement the model of Müller *et al* [46–48] and to consider the chain as an ensemble of spherical sites connected by springs. However, such modification of the theory is not simple and would imply an alteration of the 'heart' of the Yu and Wu theory [44], i.e. the scheme for the calculation of the propagator functions $G_j(z)$, equation (15). All these problems are currently under study in our laboratory. Upon finishing the manuscript we became aware of the recent work of Fu and Wu [73]. These authors used a similar (albeit more elaborate) approach to investigating the phase behaviour and interfacial tensions of low-molecular-weight normal alkanols. Using a regressed set of molecular parameters they found good agreement with experimental results over a wide range of temperatures.

Acknowledgments

We are indebted to Mark Miller for helpful comments on the manuscript. PB acknowledges financial support from the Rector of the Maria Curie-Skłodowska University, Lublin. This work was partially supported by EU TOK contract No 509249. We thank D Fu and J Wu for sending the preprint of the reference [73] prior to publication.

References

[1] Beaton C F and Hewitt G F 1989 *Physical Property Data for the Design Engineer* (New York: Hemisphere)
[2] Jasper J J 1972 *J. Phys. Chem. Ref. Data* **1** 841
[3] Wagner W and Kruse A 1998 *Properties of Water and Steam* (Berlin: Springer)
[4] Ross S and Patterson E 1979 *J. Chem. Eng. Data* **24** 111
[5] Poston R S and McKetta J J 1966 *J. Chem. Eng. Data* **11** 364
[6] Dee G T and Sauer B B 1998 *Adv. Phys.* **47** 161
[7] Jasper J J and Kring E V 1955 *J. Phys. Chem.* **59** 1019
[8] Park J and Kim H 1998 *Fluid Phase Equilib.* **150/151** 173
[9] Jain R K and Simha R 1979 *J. Chem. Phys.* **70** 5329
[10] Chandler D 1982 *Studies in Statistical Mechanics* vol 8, ed E W Montroll and J L Lebowitz (Amsterdam: North-Holland) p 275
[11] Gray C G and Gubbins K E 1984 *Theory of Molecular Fluids I. Fundamentals* (Oxford: Clarendon)
[12] Prausnitz J M, Lichtenthaler R N and Azavedo E G 1986 *Molecular Thermodynamics of Fluid Phase Equilibria* (Englewood Cliffs, NJ: Prentice-Hall)
[13] Boublik T 1970 *J. Chem. Phys.* **53** 471
[14] Lee Y P, Rangaiah G P and Chiew Y C 2001 *Fluid Phase Equilib.* **189** 135
[15] Pamies J C and Vega L F 2002 *Mol. Phys.* **100** 2519
[16] Wang X Y and Chiew Y C 2001 *J. Chem. Phys.* **115** 4376
[17] Sengers J V, Kayser R F, Peters C J and White H J 2000 *Equation of State for Fluids and Fluid Mixtures* (Amsterdam: Elsevier)
[18] Chapman W G, Gubbins K E, Jackson G and Radosz M 1989 *Fluid Phase Equilib.* **52** 31
[19] Chapman W G, Gubbins K E, Jackson G and Radosz M 1990 *Ind. Eng. Chem. Res.* **29** 1709
[20] Müller E A and Gubbins K E 2000 *Equation of State for Fluids and Fluid Mixtures* ed J V Sengers, R F Kayser, C J Peters and H J White (Amsterdam: Elsevier)
[21] Paricaud P, Galindo A and Jackson G 2002 *Fluid Phase Equilib.* **194–197** 87
[22] Huang S H and Radosz M 1990 *Ind. Eng. Chem. Res.* **29** 2284
[23] Huang S H and Radosz M 1991 *Ind. Eng. Chem. Res.* **30** 1994

[24] Wertheim M S 1987 *J. Chem. Phys.* **87** 7323
[25] Ghonasgi D and Chapman W G 1994 *J. AIChE* **40** 878
[26] Blas F J and Vega L F 1997 *Mol. Phys.* **92** 135
[27] Blas F J and Vega L F 1998 *J. Chem. Phys.* **109** 7405
[28] Blas F J and Vega L F 2000 *Fluid Phase Equilib.* **171** 91
[29] Galindo A, Gil-Villegas A, Jackson G and Burgess A N 1999 *J. Chem. Phys.* B **103** 10272
[30] McCabe C, Galindo A, Garcia-Lisbona M N and Jackson G 2001 *Ind. Eng. Chem. Res.* **40** 3835
[31] Klapp S and Forstmann F 1999 *Phys. Rev.* E **60** 3183
[32] Miqueu C, Mendiboure B, Graciaa A and Lachaise J 2003 *Fluid Phase Equilib.* **207** 225
[33] Evans R 1992 *Fundamentals of Inhomogeneous Fluids* ed D Henderson (New York: Dekker) p 85
[34] Segura C J, Chapman W G and Shukla K P 1997 *Mol. Phys.* **90** 759
[35] Borówko M, Pizio O and Sokołowski S 2000 *Computational Methods in Surface and Colloid Science* ed M Borówko (New York: Dekker) chapter 4
[36] Martinez A, Pizio O, Patrykiejew A and Sokołowski S 2003 *J. Phys.: Condens. Matter* **15** 3107
[37] Blas F, de Miguel E, Martin del Rio E and Jackson G 2001 *Mol. Phys.* **99** 1851
[38] Pizio O, Patrykiejew A and Sokołowski S 2000 *J. Chem. Phys.* **113** 10761
[39] Gloor G, Blas F, de Miguel E, Martin del Rio E and Jackson G 2002 *Fluid Phase Equilib.* **194–197** 521
[40] Borówko M, Stepniak K, Sokołowski S and Zagórski R 1999 *Czech. J. Phys.* **49** 1067
[41] Lu J F, Fu D, Liu J C and Li Y G 2002 *Fluid Phase Equilib.* **194–197** 755
[42] Peery T B and Evans G T 2001 *J. Chem. Phys.* **114** 2387
[43] Kierlik E and Rosinberg M L 1992 *J. Chem. Phys.* **97** 9222
[44] Yu Y X and Wu J 2002 *J. Chem. Phys.* **117** 2368
[45] Yu Y X and Wu J 2003 *J. Chem. Phys.* **118** 3835
[46] Müller M and MacDowell L G 2000 *Macromolecules* **33** 3902
[47] Müller M, MacDowell L G, Müller-Buschbaum P, Wunnike O and Stamm M 2001 *J. Chem. Phys.* **115** 9960
[48] Müller M, MacDowell L G and Yethiraj A 2003 *J. Chem. Phys.* **118** 2929
[49] Müller M and MacDowell L G 2003 *J. Phys.: Condens. Matter* **15** R609
[50] Gil-Villegas A, Galindo A, Whitehead P J, Mills S J and Jackson G 1997 *J. Chem. Phys.* **106** 4168
[51] MacDowell L G, Müller M, Vega C and Binder K 2000 *J. Chem. Phys.* **113** 419
[52] Bryk P and Sokołowski S 2004 *J. Chem. Phys.* **121** (21)
[53] Bryk P and Sokołowski S 2004 *J. Chem. Phys.* **120** 8299
[54] Rosenfeld Y 1989 *Phys. Rev. Lett.* **63** 980
[55] Roth R, Evans R, Lang A and Kahl G 2002 *J. Phys.: Condens. Matter* **14** 12063
[56] Yu Y X and Wu J 2002 *J. Chem. Phys.* **117** 10165
[57] Rowlinson J S 1959 *Liquids and Liquid Mixtures* (London: Butterworths)
[58] Penfold R, Abbas S and Nordholm S 1996 *Fluid Phase Equilib.* **120** 39
[59] Kleinrahm R and Wagner W 1986 *J. Chem. Thermodyn.* **18** 739
[60] Younglove B A and Ely J F 1987 *J. Phys. Chem. Ref. Data* **16** 577
[61] Daubert T E and Danner R P 1989 *Physical and Thermodynamic Properties of Pure Chemicals: Data Compilation* (Washington, DC: Taylor and Francis)
[62] Lofti A, Vrabec J and Fischer J 1992 *Mol. Phys.* **81** 1319
[63] Errington J R and Panagiotopoulos A Z 1999 *J. Phys. Chem.* B **103** 9905
[64] Wilding N B, Müller M and Binder K 1996 *J. Chem. Phys.* **105** 802
[65] Escobedo F A and de Pablo J J 1996 *Mol. Phys.* **87** 347
[66] Johnson J K, Zollweg J A and Gubbins K E 1993 *Mol. Phys.* **78** 591
[67] Kolafa J and Nezbeda I 1994 *Fluid Phase Equilib.* **100** 1
[68] Evans R, Henderson J R, Hoyle D C, Parry A O and Sabeur Z A 1993 *Mol. Phys.* **80** 755
[69] Smith P, Lynden-Bell R M and Smith W 2000 *Mol. Phys.* **98** 255
[70] Fischer J and Methfessel M 1980 *Phys. Rev.* A **22** 2836
[71] Dietrich S 1988 *Phase Transitions and Critical Phenomena* vol 12, ed C Domb and J L Lebowitz (London: Academic) p 1
[72] Alejandre J, Duda Y and Sokołowski S 2003 *J. Chem. Phys.* **118** 329
[73] Fu D and Wu J 2004 *Ind. Eng. Chem. Res.* at press